arXiv:hep-ex/0608033v2 10 Feb 2007

# Improved Measurements of Branching Fractions and $CP$ Asymmetries in $B \to \eta h$ Decays


P. Chang,[24] K. Abe,[40] I. Adachi,[7] H. Aihara,[42] D. Anipko,[1] A. M. Bakich,[38] E. Barberio,[19] A. Bay,[17] U. Bitenc,[13] I. Bizjak,[13] A. Bondar,[1] A. Bozek,[25] M. Bračko,[7,18,13] T. E. Browder,[6] Y. Chao,[24] A. Chen,[22] K.-F. Chen,[24] W. T. Chen,[22] B. G. Cheon,[3] R. Chistov,[12] S.-K. Choi,[48] Y. Choi,[37] Y. K. Choi,[37] S. Cole,[38] J. Dalseno,[19] M. Dash,[46] J. Dragic,[7] S. Eidelman,[1] S. Fratina,[13] N. Gabyshev,[1] A. Go,[22] A. Gorišek,[13] H. Ha,[15] J. Haba,[7] K. Hara,[20] H. Hayashii,[21] M. Hazumi,[7] D. Heffernan,[30] T. Hokuue,[20] Y. Hoshi,[40] S. Hou,[22] W.-S. Hou,[24] T. Iijima,[20] K. Inami,[20] A. Ishikawa,[42] H. Ishino,[43] R. Itoh,[7] M. Iwasaki,[42] Y. Iwasaki,[7] H. Kaji,[20] J. H. Kang,[47] S. U. Kataoka,[21] H. Kawai,[2] T. Kawasaki,[27] H. Kichimi,[7] H. J. Kim,[16] Y. J. Kim,[5] K. Kinoshita,[4] S. Korpar,[18,13] P. Krokovny,[7] R. Kumar,[31] C. C. Kuo,[22] A. Kuzmin,[1] Y.-J. Kwon,[47] M. J. Lee,[35] S. E. Lee,[35] T. Lesiak,[25] S.-W. Lin,[24] F. Mandl,[10] T. Matsumoto,[44] S. McOnie,[38] H. Miyata,[27] Y. Miyazaki,[20] R. Mizuk,[12] G. R. Moloney,[19] T. Mori,[20] Y. Nagasaka,[8] M. Nakao,[7] S. Nishida,[7] O. Nitoh,[45] S. Ogawa,[39] T. Ohshima,[20] S. Okuno,[14] Y. Onuki,[33] H. Ozaki,[7] P. Pakhlov,[12] G. Pakhlova,[12] H. Park,[16] L. S. Peak,[38] R. Pestotnik,[13] L. E. Piilonen,[46] Y. Sakai,[7] N. Satoyama,[36] T. Schietinger,[17] O. Schneider,[17] J. Schümann,[7] C. Schwanda,[10] A. J. Schwartz,[4] K. Senyo,[20] M. E. Sevior,[19] M. Shapkin,[11] H. Shibuya,[39] B. Shwartz,[1] J. B. Singh,[31] A. Somov,[4] N. Soni,[31] S. Stanič,[28] M. Starič,[13] H. Stoeck,[38] T. Sumiyoshi,[44] F. Takasaki,[7] M. Tanaka,[7] G. N. Taylor,[19] Y. Teramoto,[29] X. C. Tian,[32] I. Tikhomirov,[12] K. Trabelsi,[7] T. Tsuboyama,[7] T. Tsukamoto,[7] S. Uehara,[7] T. Uglov,[12] K. Ueno,[24] Y. Unno,[3] S. Uno,[7] Y. Usov,[1] G. Varner,[6] K. E. Varvell,[38] S. Villa,[17] C. C. Wang,[24] C. H. Wang,[23] M.-Z. Wang,[24] M. Watanabe,[27] Y. Watanabe,[43] R. Wedd,[19] J. Wicht,[17] E. Won,[15] A. Yamaguchi,[41] Y. Yamashita,[26] M. Yamauchi,[7] C. C. Zhang,[9] Z. P. Zhang,[34] V. Zhilich,[1] and A. Zupanc[13]

(The Belle Collaboration)

[1]*Budker Institute of Nuclear Physics, Novosibirsk*
[2]*Chiba University, Chiba*
[3]*Chonnam National University, Kwangju*
[4]*University of Cincinnati, Cincinnati, Ohio 45221*
[5]*The Graduate University for Advanced Studies, Hayama, Japan*
[6]*University of Hawaii, Honolulu, Hawaii 96822*
[7]*High Energy Accelerator Research Organization (KEK), Tsukuba*
[8]*Hiroshima Institute of Technology, Hiroshima*
[9]*Institute of High Energy Physics, Chinese Academy of Sciences, Beijing*
[10]*Institute of High Energy Physics, Vienna*
[11]*Institute of High Energy Physics, Protvino*
[12]*Institute for Theoretical and Experimental Physics, Moscow*
[13]*J. Stefan Institute, Ljubljana*
[14]*Kanagawa University, Yokohama*
[15]*Korea University, Seoul*
[16]*Kyungpook National University, Taegu*
[17]*Swiss Federal Institute of Technology of Lausanne, EPFL, Lausanne*
[18]*University of Maribor, Maribor*
[19]*University of Melbourne, Victoria*
[20]*Nagoya University, Nagoya*
[21]*Nara Women's University, Nara*
[22]*National Central University, Chung-li*
[23]*National United University, Miao Li*
[24]*Department of Physics, National Taiwan University, Taipei*
[25]*H. Niewodniczanski Institute of Nuclear Physics, Krakow*
[26]*Nippon Dental University, Niigata*
[27]*Niigata University, Niigata*
[28]*University of Nova Gorica, Nova Gorica*
[29]*Osaka City University, Osaka*
[30]*Osaka University, Osaka*
[31]*Panjab University, Chandigarh*
[32]*Peking University, Beijing*

[33]RIKEN BNL Research Center, Upton, New York 11973
[34]University of Science and Technology of China, Hefei
[35]Seoul National University, Seoul
[36]Shinshu University, Nagano
[37]Sungkyunkwan University, Suwon
[38]University of Sydney, Sydney NSW
[39]Toho University, Funabashi
[40]Tohoku Gakuin University, Tagajo
[41]Tohoku University, Sendai
[42]Department of Physics, University of Tokyo, Tokyo
[43]Tokyo Institute of Technology, Tokyo
[44]Tokyo Metropolitan University, Tokyo
[45]Tokyo University of Agriculture and Technology, Tokyo
[46]Virginia Polytechnic Institute and State University, Blacksburg, Virginia 24061
[47]Yonsei University, Seoul
[48]Gyeongsang National University, Chinju

We report improved measurements of $B$ decays with an $\eta$ meson in the final state using 492 fb$^{-1}$ of data collected by the Belle detector at the KEKB $e^+e^-$ collider. We observe the decays $B^\pm \to \eta\pi^\pm$ and $B^\pm \to \eta K^\pm$ and measure the branching fractions $\mathcal{B}(B^\pm \to \eta\pi^\pm) = (4.2 \pm 0.4(\mathrm{stat}) \pm 0.2(\mathrm{sys})) \times 10^{-6}$ and $\mathcal{B}(B^\pm \to \eta K^\pm) = (1.9 \pm 0.3(\mathrm{stat})^{+0.2}_{-0.1}(\mathrm{sys})) \times 10^{-6}$. The corresponding $CP$-violating asymmetries are measured to be $-0.23 \pm 0.09(\mathrm{stat}) \pm 0.02(\mathrm{sys})$ for $\eta\pi^\pm$ and $-0.39 \pm 0.16(\mathrm{stat}) \pm 0.03(\mathrm{sys})$ for $\eta K^\pm$. We also search for $B^0 \to \eta K^0$ decays and set an upper limit of $1.9 \times 10^{-6}$ at the 90% confidence level.

PACS numbers: 13.25.Hw, 12.15.Hh, 11.30.Er

Charmless $B$ decays provide a rich sample to understand $B$ decay dynamics and to search for $CP$ violation. The decay $B \to \eta K$ proceeds through a $b \to s$ penguin process and a $b \to u$ tree transition. Interference from the two penguin processes, $b \to s\overline{s}s$ and $b \to u\overline{u}s$, and the known $\eta - \eta'$ mixing are expected to enhance the $B \to \eta' K$ branching fraction but suppress $B \to \eta K$ [1]. The situation is reversed for the $\eta K^*$ and $\eta' K^*$ modes since the $\eta$ and $K^*$ mesons are in a relative p-wave rather than an s-wave state. Experimental results [2, 3, 4, 5] have confirmed this picture but more precise measurements of $\eta K$ and $\eta' K^*$ are needed for a quantitative understanding of the underlying dynamics. Moreover, the penguin amplitude of $\eta K$ may interfere with the $b \to u$ amplitude, resulting in a large direct $CP$ asymmetry ($A_{CP}$) [6]. Theoretical expectations for contributions from other mechanisms [7, 8, 9] also suggest a large $A_{CP}$ although the sign could be positive or negative. Our earlier measurements with limited statistics [3] indicated a large negative $A_{CP}$ central value for $\eta K^\pm$.

The study of $B^0 \to \eta K^0$ is of particular interest because this decay is a $CP$ eigenstate and could be used for time dependent $CP$ measurements. The dominant process in $B \to \eta\pi$ decays is the (external) $b \to u$ tree while a suppressed $b \to d$ penguin process may also contribute. It has been argued [7, 10] that the direct $CP$ violating asymmetry could be large in the $\eta\pi^\pm$ and $\eta'\pi^\pm$ modes, whose branching fractions are expected to be around $(2-5) \times 10^{-6}$ [9, 10].

In this paper, we report improved measurements of branching fractions and partial rate asymmetries for $B \to \eta h$ decays, where $h$ is a charged or neutral $K$ meson or a charged $\pi$ meson. The partial rate asymmetry for charged $B$ decays is defined to be:

$$A_{CP} = \frac{N(B^- \to \eta h^-) - N(B^+ \to \eta h^+)}{N(B^- \to \eta h^-) + N(B^+ \to \eta h^+)}, \qquad (1)$$

where $N(B^- \to \eta h^-)$ is the yield obtained for the $B^- \to \eta h^-$ decay and $N(B^+ \to \eta h^+)$ denotes that of the charge-conjugate mode. The data sample consists of 535 million $B\overline{B}$ pairs (492 fb$^{-1}$) collected with the Belle detector at the KEKB $e^+e^-$ asymmetric-energy (3.5 on 8 GeV) collider [11] operating at the $\Upsilon(4S)$ resonance. Throughout this paper, the inclusion of the charge-conjugate decay mode is implied unless otherwise stated.

The Belle detector is a large-solid-angle magnetic spectrometer that consists of a silicon vertex detector (SVD), a 50-layer central drift chamber (CDC), an array of aerogel threshold Čerenkov counters (ACC), a barrel-like arrangement of time-of-flight scintillation counters (TOF), and an electromagnetic calorimeter (ECL) comprised of CsI(Tl) crystals located inside a superconducting solenoid coil that provides a 1.5 T magnetic field. An iron flux-return located outside the coil is instrumented to detect $K_L^0$ mesons and to identify muons (KLM). The detector is described in detail elsewhere [12]. In August 2003, the three-layer SVD was replaced by a four-layer device with greater radiation tolerance [13]. The data sample used in this analysis consists of 140 fb$^{-1}$ of data with the old SVD (Set I) and 352 fb$^{-1}$ with the new one (Set II).

The event selection and $B$ candidate reconstruction are similar to those documented in our previous publication

[3]. Two $\eta$ decay channels are considered in this analysis: $\eta \to \gamma\gamma$ ($\eta_{\gamma\gamma}$) and $\eta \to \pi^+\pi^-\pi^0$ ($\eta_{3\pi}$). We require photons from the $\eta$ and $\pi^0$ candidates to have laboratory energies ($E_\gamma$) above 50 MeV. In the $\eta_{\gamma\gamma}$ reconstruction, the photon energy asymmetry, $\frac{|E_{\gamma 1}-E_{\gamma 2}|}{E_{\gamma 1}+E_{\gamma 2}}$, is required to be less than 0.9 to reduce the large combinatorial background from soft photons. Neither photon from $\eta_{\gamma\gamma}$ is allowed to pair with any other photon having $E_\gamma > 100$ MeV to form a $\pi^0$ candidate. Candidate $\pi^0$ mesons are selected by requiring the two-photon invariant mass to be in a mass window between 115 MeV/$c^2$ and 152 MeV/$c^2$. The momentum vector of each photon is then readjusted to constrain the mass of the photon pair to the nominal $\pi^0$ mass.

Candidate $\eta_{3\pi}$ mesons are reconstructed by combining $\pi^0$ candidates with at least 250 MeV/$c$ laboratory momentum with a pair of oppositely charged tracks that originate from the interaction point (IP). We impose the following requirements on the invariant mass of the $\eta$ candidates in both data sets: 516 MeV/$c^2 < M_{\gamma\gamma} <$ 569 MeV/$c^2$ for $\eta_{\gamma\gamma}$ and 539 MeV/$c^2 < M_{3\pi} <$ 556 MeV/$c^2$ for $\eta_{3\pi}$. After the selection of each candidate, the $\eta$ mass constraint is implemented by readjusting the momentum vectors of the daughter particles.

Charged tracks are required to come from the IP. Charged kaons and pions, which are combined with $\eta$ mesons to form $B$ candidates, are identified using a $K(\pi)$ likelihood $L_K(L_\pi)$ obtained by combining information from the CDC ($dE/dx$), the TOF and the ACC. Discrimination between kaons and pions is achieved through a requirement on the likelihood ratio $L_K/(L_\pi + L_K)$. Charged tracks with likelihood ratios greater than 0.6 are regarded as kaons, and less than 0.4 as pions. Charged tracks that are positively identified as electrons or muons are rejected. The $K/\pi$ identification efficiencies (PID) and misidentification rates are determined from a sample of $D^{*+} \to D^0\pi^+, D^0 \to K^-\pi^+$ decays with kaons and pions in the same kinematic region of two-body $B$ decays. The kaon (pion) identification efficiency is 83% (90%) and 6.4% (11.7%) of pions (kaons) will be misidentified as kaons (pions). The systematic error of the $K/\pi$ selection is about 1.3% for pions and 1.5% for kaons, respectively.

$K_S^0$ candidates are reconstructed from pairs of oppositely-charged tracks with an invariant mass ($M_{\pi\pi}$) between 480 MeV/$c^2$ and 516 MeV/$c^2$. Each candidate must have a displaced vertex with a flight direction consistent with that of a $K_S^0$-meson originating from the IP.

Candidate $B$ mesons are identified using the beam-energy constrained mass, $M_{\rm bc} = \sqrt{E_{\rm beam}^2 - P_B^2}$, and the energy difference, $\Delta E = E_B - E_{\rm beam}$, where $E_{\rm beam}$ is the run-dependent beam energy in the $\Upsilon(4S)$ rest frame determined from $B \to D^{(*)}\pi$ events, and $P_B$ and $E_B$ are the momentum and energy, respectively of the $B$ candidate in the $\Upsilon(4S)$ rest frame. The resolutions in $M_{\rm bc}$ and $\Delta E$ are about 3 MeV/$c^2$ and 20–30 MeV, respectively. Events with $M_{\rm bc} > 5.2$ GeV/$c^2$ and $|\Delta E| < 0.3$ GeV are selected for the analysis.

The dominant background comes from the $e^+e^- \to q\bar{q}$ continuum, where $q = u, d, s$ or $c$. To distinguish signal from the jet-like continuum background, event shape variables and $B$ flavor tagging information are employed. We combine the correlated shape variables into a Fisher discriminant [14] and then compute a likelihood that is the product of probabilities based on this discriminant and $\cos\theta_B$, where $\theta_B$ is the angle between the $B$ flight direction and the beam direction in the $\Upsilon(4S)$ rest frame. A likelihood ratio, $\mathcal{R} = \mathcal{L}_s/(\mathcal{L}_s + \mathcal{L}_{q\bar{q}})$, is formed from signal ($\mathcal{L}_s$) and background ($\mathcal{L}_{q\bar{q}}$) likelihoods, obtained from Monte Carlo simulation (MC) and from data with $M_{\rm bc} < 5.26$ GeV/$c^2$, respectively. Signal MC events for the charged $B$ modes are generated with the PHOTOS [15] simulation package to take into account final state radiation. Additional background discrimination is provided by $B$ flavor tagging. Events that contain a lepton (such as those used in high quality tagging) are more likely to be $B\overline{B}$ events so a looser $\mathcal{R}$ requirement is applied. The standard Belle $B$ tagging package [16] provides two outputs: a discrete variable ($q$) indicating the tagged side flavor and a dilution factor ($r$) ranging from zero for no flavor information to unity for unambiguous flavor assignment. Since the charged $B$ modes are flavor specific, the wrong flavor tagged events are likely to be background and a tight $\mathcal{R}$ requirement can be applied. We divide the data into six sub-samples based on the $q$ and $r$ information for the charged modes and the $r$ value only for the neutral mode. Continuum suppression is achieved by applying a mode-dependent requirement on $\mathcal{R}$ for events in each sub-sample that maximizes $N_s^{\rm exp}/\sqrt{N_s^{\rm exp} + N_{q\bar{q}}^{\rm exp}}$, where $N_s^{\rm exp}$ is the number of signal events expected from MC and $N_{q\bar{q}}^{\rm exp}$ denotes the number of background events estimated from data. After applying the $\mathcal{R}$ requirements, we select one candidate per event based on the best $\mathcal{R}$. The fraction of events with multiple candidates are $\sim 1\%$ for the $\gamma\gamma$ mode and $\sim$2-3% for the $\pi^+\pi^-\pi^0$ mode.

Using a large MC sample, all other backgrounds are found to be negligible except for $\eta K^+(\eta\pi^+)$ reflecting into the $\eta\pi^+(\eta K^+)$ sample, due to $K^+ \to \pi^+(\pi^+ \to K^+)$ misidentification, and the feed-down from charmless $B$ decays, predominantly $B \to \eta K^*(892)$ and $B \to \eta\rho(770)$. We include the reflection and charmless components in the fit used to extract the signal.

The signal yields and partial rate asymmetries are obtained using an extended unbinned maximum-likelihood (ML) fit with input variables $M_{\rm bc}$ and $\Delta E$. The likeli-

hood is defined as:

$$\mathcal{L} = e^{-\sum_j N_j} \times \prod_i (\sum_j N_j \mathcal{P}_j^i) \quad \text{and} \tag{2}$$

$$\mathcal{P}_j^i = \frac{1}{2}[1 - q^i \cdot A_{CP\,j}] P_j(M_{\rm bc}^i, \Delta E^i), \tag{3}$$

where $i$ is the identifier of the $i$-th event and $N_j$ is the number of events for the category $j$, which corresponds to either signal, $q\bar{q}$ continuum, the reflection due to $K$-$\pi$ misidentification, or background from other charmless $B$ decays. $P_j(M_{\rm bc}, \Delta E)$ is the two-dimensional probability density function (PDF) in $M_{\rm bc}$ and $\Delta E$, and $q$ indicates the $B$ meson flavor, $B^+(q = +1)$ or $B^-(q = -1)$. For the neutral $B$ mode, $\mathcal{P}_j^i$ in Eq. 2 is simply $P_j(M_{\rm bc}^i, \Delta E^i)$ and there is no component from charged particle misidentification.

In Ref. [17] we reported that in both data sets the PID efficiency is slightly different for positively and negatively charged particles. Therefore, the raw asymmetry defined in Eq. 1 must be corrected. This efficiency difference results in an $A_{CP}$ bias of $-0.005$ ($+0.005$) for $\eta\pi$ ($\eta K$). The bias is subtracted from the raw asymmetry.

The PDFs for the signal, the reflection background and the charmless feed-down are modeled with two-dimensional $M_{\rm bc}$-$\Delta E$ smooth functions obtained using large MC samples. The signal peak positions and resolutions in $M_{\rm bc}$ and $\Delta E$ are adjusted according to the data-MC differences using large control samples of $B \to D\pi$ and $\overline{D}^0 \to K^+\pi^-\pi^0$ decays. The continuum background in $\Delta E$ is described by a first- or second-order polynomial, while the $M_{\rm bc}$ distribution is parameterized by an ARGUS function, $f(x) = x\sqrt{1-x^2}\exp[-\xi(1-x^2)]$, where $x$ is $M_{\rm bc}/E_{\rm beam}$ [18]. The continuum PDF is thus formed by the product of an ARGUS function and a polynomial, where $\xi$ and the coefficients of the polynomial are free parameters.

The partial rate asymmetries of the charmless $B$ backgrounds are fixed to zero in the fit while the $A_{CP}$ and normalizations of the reflection components are fixed to expectations based on the $B^+ \to \eta K^+$ and $B^+ \to \eta\pi^+$ partial rate asymmetries and branching fractions, as well as $K^+ \leftrightarrow \pi^+$ fake rates. The reflection yield and $A_{CP}$ are first input with the assumed values and are then recalculated according to our measured results.

Table I shows the measured branching fractions for each decay mode as well as other quantities associated with the measurements. The efficiency for each mode is determined using MC simulation and corrected for the data-MC discrepancy obtained from the control sample studies. In addition to the particle identification performance discrepancy, our MC slightly overestimates the efficiency for detecting low momentum $\pi^0$s, which results in a 3.1% correction for the $\eta_{3\pi}$ mode. The combined branching fraction for the two datasets is computed as the sum of the yield divided by its efficiency in each set divided by the number of $B$ mesons, while the partial rate asymmetry for the charged mode is computed using the sum of the yield divided by its efficiency in each set in Eq. 1. The combined branching fraction and partial rate asymmetry of the two $\eta$ decay modes are obtained from the weighted average assuming the errors are Gaussian. The number of $B^+B^-$ and $B^0\overline{B}^0$ pairs are assumed to be equal. Figure 1 shows the $M_{\rm bc}$ and $\Delta E$ projections after requiring events to satisfy $-0.10$ GeV $< \Delta E < 0.08$ GeV and $M_{\rm bc} > 5.27$ GeV/$c^2$, respectively.

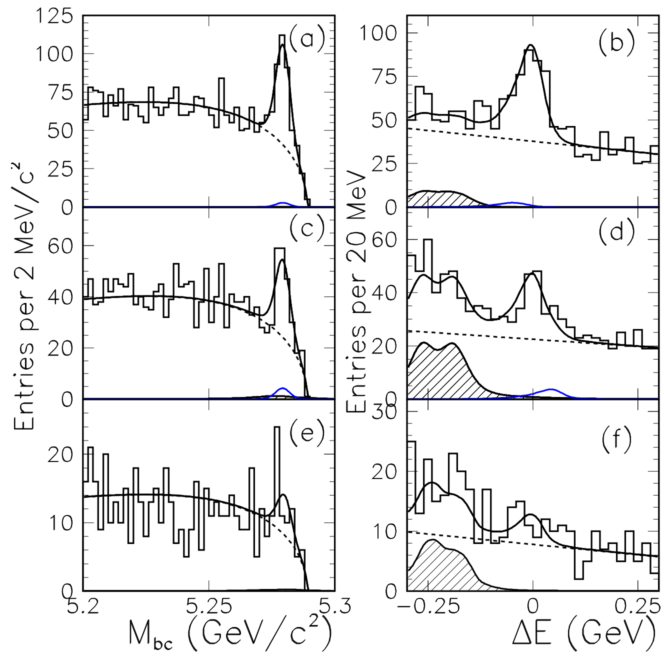


FIG. 1: $M_{\rm bc}$ and $\Delta E$ projections for (a,b) $B^\pm \to \eta\pi^\pm$, (c,d) $B^\pm \to \eta K^\pm$, and (e,f) $B^0 \to \eta K^0$ decays with the $\eta_{\gamma\gamma}$ and $\eta_{3\pi}$ modes combined. Open histograms are data, solid curves are the fit functions, dashed lines show the continuum contributions and shaded histograms are the feed-down component from charmless $B$ decays. The small contributions around $M_{\rm bc} = 5.28$ GeV/$c^2$ and $\Delta E = \pm 0.05$ GeV in (a)-(d) are the reflection backgrounds from $B^\pm \to \eta K^\pm$ and $B^\pm \to \eta\pi^\pm$.

Systematic uncertainties due to the signal PDFs used in the fit are estimated by performing the fit after varying the signal peak positions and resolutions by one standard deviation ($\sigma$). We also examine the changes in yield and $A_{CP}$ when the requirement of no asymmetry for the charmless background is removed. In $B^\pm \to \eta\pi^\pm$, the reflection yields are estimated to be $9.4 \pm 3.1$ events for the $\eta_{\gamma\gamma}$ mode and $3.6 \pm 1.9$ for $\eta_{3\pi}$ while in $B^\pm \to \eta K^\pm$, the reflection yields are $13.9 \pm 3.7$ for $\eta_{\gamma\gamma}$ and $4.6 \pm 2.1$ for $\eta_{3\pi}$. The reflection yields and their $A_{CP}$ values are varied by one standard deviation in the fit to obtain the corresponding systematic uncertainties. The quadratic sum of the deviations from the central value gives the systematic uncertainty in the fit. A statistical significance is calculated as $\mathcal{S} = \sqrt{-2\ln\mathcal{L}_0 - (-2\ln\mathcal{L}_{\rm max})}$, where $-2\ln\mathcal{L}_0$ is for zero signal yield and $-2\ln\mathcal{L}_{\rm max}$ is for the best-fit value. The final significance including systematic uncer-

TABLE I: Detection efficiency ($\epsilon$) including sub-decay branching fraction [19], yield, significance (Sig.), measured branching fraction ($\mathcal{B}$), the 90% C.L. upper limit (UL) and $A_{CP}$ for the $B \to \eta h$ decays. The first errors in columns 3, 5 and 7 are statistical and the second errors are systematic.

| Mode | $\epsilon$(%) | Yield | Sig. | $\mathcal{B}(10^{-6})$ | UL$(10^{-6})$ | $A_{CP}$ |
|---|---|---|---|---|---|---|
| $B^{\pm} \to \eta\pi^{\pm}$ | | | 14.7 | $4.2 \pm 0.4 \pm 0.2$ | | $-0.23 \pm 0.09 \pm 0.02$ |
| $\eta_{\gamma\gamma}\pi^{\pm}$ | 8.3 | $183 \pm 20$ | 11.9 | $4.1^{+0.5}_{-0.4} \pm 0.2$ | | $-0.11 \pm 0.11 \pm 0.01$ |
| $\eta_{3\pi}\pi^{\pm}$ | 3.1 | $73^{+13}_{-12}$ | 8.7 | $4.4^{+0.8}_{-0.7} \pm 0.3$ | | $-0.52 \pm 0.16 \pm 0.02$ |
| $B^{\pm} \to \eta K^{\pm}$ | | | 8.1 | $1.9 \pm 0.3^{+0.2}_{-0.1}$ | | $-0.39 \pm 0.16 \pm 0.03$ |
| $\eta_{\gamma\gamma}K^{\pm}$ | 7.3 | $72^{+14}_{-13}$ | 6.4 | $1.9^{+0.4}_{-0.3} \pm 0.1$ | | $-0.30 \pm 0.19 \pm 0.02$ |
| $\eta_{3\pi}K^{\pm}$ | 2.7 | $29 \pm 8$ | 4.8 | $2.0^{+0.6}_{-0.4} \pm 0.2$ | | $-0.55^{+0.27+0.05}_{-0.28-0.04}$ |
| $B^0 \to \eta K^0$ | | | 2.9 | $1.1 \pm 0.4 \pm 0.1$ | $< 1.9$ | |
| $\eta_{\gamma\gamma}K^0$ | 2.6 | $16 \pm 8$ | 2.6 | $1.1^{+0.6}_{-0.5} \pm 0.1$ | $< 2.2$ | |
| $\eta_{3\pi}K^0$ | 1.0 | $4.6^{+4.6}_{-3.7}$ | 1.2 | $0.9^{+0.9}_{-0.7} \pm 0.1$ | $< 2.4$ | |

tainty is taken as $\mathcal{S} = \mathcal{S}_o - \sqrt{\Sigma(\mathcal{S}_o - \mathcal{S}_i)^2}$, where $\mathcal{S}_o$ is the statistical significance for the fit and $\mathcal{S}_i$ is the significance obtained for each systematic check with the value smaller than $\mathcal{S}_o$.

The possible detector bias due to the tracking acceptance for $A_{CP}(B^{\pm} \to \eta\pi^{\pm})$ and $A_{CP}(B^{\pm} \to \eta K^{\pm})$ is evaluated using the $A_{CP}$ value of the continuum component. No obvious bias is observed and we use the statistical error of the $\eta_{\gamma\gamma}$ and $\eta_{3\pi}$ modes combined as the systematic error. The bias error of 0.01 is added in quadrature with the fit systematic error to give the final systematic uncertainty in Table I. Figures 2 and 3 show the $M_{\rm bc}$ and $\Delta E$ projections for the $B^+$ and $B^-$ samples. In both the $\eta\pi^{\pm}$ and $\eta K^{\pm}$ modes, we observe larger $B^+$ signals.

The systematic error of the efficiency arises from the $\mathcal{R}$ requirement, tracking efficiency, particle identification, $K_S^0$ reconstruction, $\pi^0$ and $\eta_{\gamma\gamma}$ reconstruction, and $\eta_{\gamma\gamma}$ and $\eta_{3\pi}$ branching fractions. The performance of the $\mathcal{R}$ requirement is studied by checking the data-MC efficiency ratio using the $B^+ \to \overline{D}{}^0\pi^+$ control sample. The systematic errors on the charged track reconstruction are estimated to be 1% per track using partially reconstructed $D^*$ events. The $\pi^0$ and $\eta_{\gamma\gamma}$ reconstruction efficiency is verified by comparing the $\pi^0$ decay angular distribution with the MC prediction, and by measuring the ratio of the branching fractions for the two $D$ decay channels $\overline{D}{}^0 \to K^+\pi^-$ and $\overline{D}{}^0 \to K^+\pi^-\pi^0$. The $K_S^0$ reconstruction is verified by comparing the ratio of $D^+ \to K_S^0\pi^+$ and $D^+ \to K^-\pi^+\pi^+$ yields. The uncertainties in the $\eta_{\gamma\gamma}$ and $\eta_{3\pi}$ branching fractions are taken from Ref. [19]. Table II summarizes the systematic uncertainties, including the error on the number of $B\overline{B}$ events. The systematic error that arises from how well PHOTOS describes final state radiation is found to be negligible [20]. The final systematic error for the combined branching fraction is obtained by assuming that the systematic errors for the sub-decay modes are 100% correlated.

We observe an excess of $B^0 \to \eta K^0$ events but the

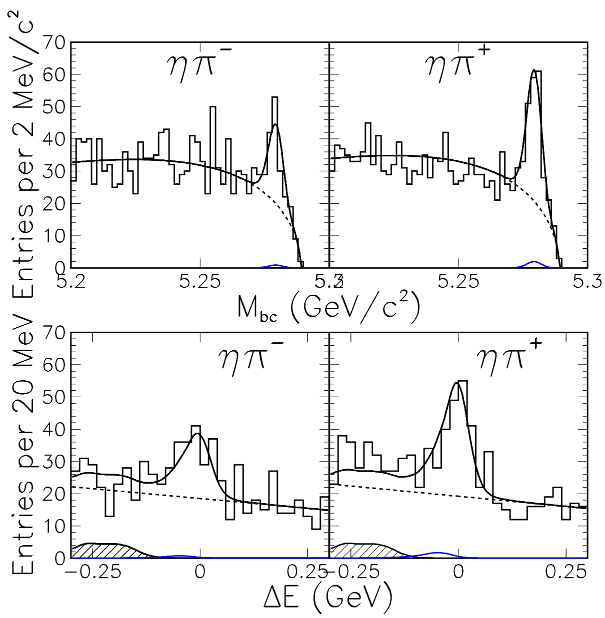


FIG. 2: $M_{\rm bc}$ and $\Delta E$ projections for (left) $B^- \to \eta\pi^-$ and (right) $B^+ \to \eta\pi^+$ with the $\eta_{\gamma\gamma}$ and $\eta_{3\pi}$ modes combined. Open histograms are data, solid curves are the fit functions, dashed lines show the continuum contributions and shaded histograms are the contributions from charmless $B$ decays. The small contributions near $M_{\rm bc} = 5.28$ GeV/$c^2$ and $\Delta E = -0.05$ GeV are the backgrounds from misidentified $B^{\pm} \to \eta K^{\pm}$ (reflections).

significance is slightly less than 3. Therefore, an upper limit on the branching fraction at 90% confidence level is provided. To calculate this limit, we find the yield for which 90% of the area of the likelihood function lies at lower values. We divide the yield by the reconstruction efficiency reduced by $1\sigma$ of its uncertainty, which is the quadratic sum of the errors given in Rows 2-8 of Table 2. The result is then inflated by the $1\sigma$ uncertainty due to the parameters fixed in the fit (1st row of Table 2) to obtain the upper limit including all systematic uncertainties.

TABLE II: The systematic uncertainties for the $B \to \eta h$ branching fractions, given in %. The fit systematic errors include the uncertainties due to the signal PDFs, the yields of the reflection backgrounds and the partial rate asymmetries of the charmless $B$ and reflection backgrounds.

| Sources | $\eta_{\gamma\gamma}\pi^\pm$ | $\eta_{3\pi}\pi^\pm$ | $\eta_{\gamma\gamma}K^\pm$ | $\eta_{3\pi}K^\pm$ | $\eta_{\gamma\gamma}K^0$ | $\eta_{3\pi}K^0$ |
|---|---|---|---|---|---|---|
| Fit | $^{+2.6}_{-3.0}$ | $^{+3.0}_{-3.6}$ | $^{+6.1}_{-4.3}$ | $^{+6.2}_{-6.4}$ | $^{+6.0}_{-6.2}$ | $\pm6.7$ |
| $\mathcal{R}$ requirement | $\pm1.2$ | $\pm1.2$ | $\pm1.2$ | $\pm1.6$ | $\pm1.4$ | $\pm1.4$ |
| Tracking | $\pm1.0$ | $\pm3.0$ | $\pm1.0$ | $\pm3.0$ | – | $\pm2.0$ |
| PID | $\pm1.3$ | $\pm1.3$ | $\pm1.5$ | $\pm1.5$ | – | – |
| $K_S^0$ reconstruction | – | – | – | – | $\pm4.9$ | $\pm4.9$ |
| $\gamma\gamma$ reconstruction | $\pm4.0$ | $\pm4.0$ | $\pm4.0$ | $\pm4.0$ | $\pm4.0$ | $\pm4.0$ |
| $\mathcal{B}(\eta \to \gamma\gamma)$ | $\pm0.7$ | – | $\pm0.7$ | – | $\pm0.7$ | – |
| $\mathcal{B}(\eta \to \pi^+\pi^-\pi^0)$ | – | $\pm1.8$ | – | $\pm1.8$ | – | $\pm1.8$ |
| $N_B$ | $\pm1.3$ | $\pm1.3$ | $\pm1.3$ | $\pm1.3$ | $\pm1.3$ | $\pm1.3$ |
| Sum | $^{+5.4}_{-5.6}$ | $^{+6.5}_{-6.6}$ | $^{+7.7}_{-6.4}$ | $^{+8.5}_{-8.7}$ | $^{+8.9}_{-9.1}$ | $\pm9.8$ |

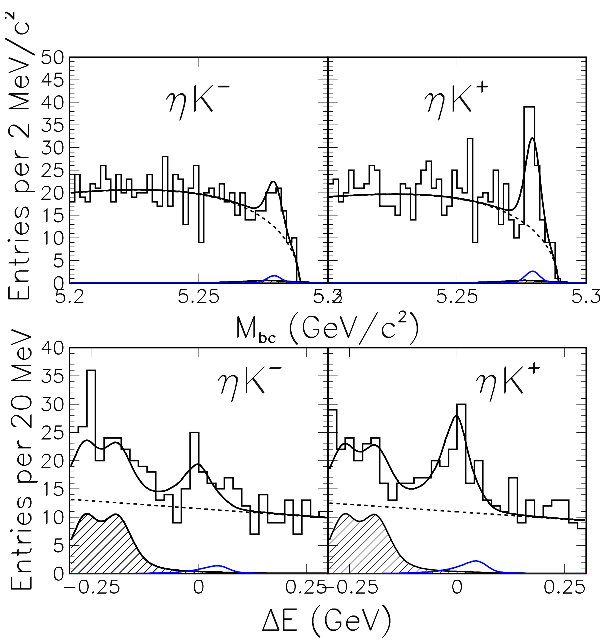


FIG. 3: $M_{\rm bc}$ and $\Delta E$ projections for (left) $B^- \to \eta K^-$ and (right) $B^+ \to \eta K^+$ with the $\eta_{\gamma\gamma}$ and $\eta_{3\pi}$ modes combined. All symbols are the same as in Fig. 2. The small contributions near $M_{\rm bc} = 5.28$ GeV/$c^2$ and $\Delta E = 0.05$ GeV are the backgrounds from misidentified $B^\pm \to \eta\pi^\pm$ (reflections).

In summary, we have observed $B^\pm \to \eta\pi^\pm$ and $B^\pm \to \eta K^\pm$ decays; their branching fractions are measured to be $(4.2 \pm 0.4 \pm 0.2) \times 10^{-6}$ and $(1.9 \pm 0.3^{+0.2}_{-0.1}) \times 10^{-6}$, respectively. These results are consistent with our previously published measurements [3] with statistical errors reduced by more than 40%. Compared with the earlier BaBar results [4], our measurements are more precise despite a $1.8\sigma$ lower branching fraction on $B^\pm \to \eta K^\pm$. The $CP$-violating asymmetries are measured to be $A_{CP}(B^\pm \to \eta\pi^\pm) = -0.23 \pm 0.09 \pm 0.02$ and $A_{CP}(B^\pm \to \eta K^\pm) = -0.39 \pm 0.16 \pm 0.03$, which are $2.5\sigma$ and $2.4\sigma$ away from zero, respectively. It is interesting to note that the $A_{CP}$ values for these two modes obtained by the BaBar collaboration are also negative, slightly more than $1\sigma$ away from zero for each mode. Larger data samples are needed to verify these large $CP$ asymmetries. Finally, we find a hint of an $\eta K^0$ signal with $\mathcal{B}(B^0 \to \eta K^0) = (1.1 \pm 0.4 \pm 0.1) \times 10^{-6}$. Since the measurement is not significant, we provide an upper limit at the 90% confidence level of $1.9 \times 10^{-6}$. A similar hint was also observed by the BaBar collaboration with a central value of $(1.5 \pm 0.7 \pm 0.1) \times 10^{-6}$. The combined average, $(1.2 \pm 0.4) \times 10^{-6}$, shows $3.4\sigma$ evidence for the $CP$ eigenstate decay $B^0 \to \eta K^0$.

We thank the KEKB group for the excellent operation of the accelerator, the KEK Cryogenics group for the efficient operation of the solenoid, and the KEK computer group and the NII for valuable computing and Super-SINET network support. We acknowledge support from MEXT and JSPS (Japan); ARC and DEST (Australia); NSFC (contract No. 10175071, China); DST (India); the BK21 program of MOEHRD and the CHEP SRC program of KOSEF (Korea); KBN (contract No. 2P03B 01324, Poland); MIST (Russia); MESS (Slovenia); NSC and MOE (Taiwan); and DOE (USA).

[1] H. J. Lipkin, Phys. Lett. B **254**, 247 (1991).

[2] CLEO Collaboration, S. J. Richichi *et al.*, Phys. Rev. Lett. **85**, 520 (2000); BaBar Collaboration, B. Aubert *et al.*, Phys. Rev. Lett. **94**, 191802 (2005); Belle Collaboration, J. Schuemann *et al.*, Phys. Rev. Lett. **97**, 061802 (2006).

[3] Belle Collaboration, P. Chang *et al.*, Phys. Rev. D **71**, 091106(R) (2005).

[4] BaBar Collaboration, B. Aubert *et al.*, Phys. Rev. Lett. **95**, 131803 (2005); BaBar Collaboration, B. Aubert *et al.*, Phys. Rev. D **70**, 032006 (2004).

[5] BaBar Collaboration, B. Aubert *et al.*, Phys. Rev. Lett. **97**, 201802 (2006).

[6] M. Bander, D. Silverman and A. Soni, Phys. Rev. Lett. **43**, 242 (1979).

[7] M.-Z. Yang and Y.-D. Yang, Nucl. Phys. B **609**, 469

(2001).
[8] M. Beneke and M. Neubert, Nucl. Phys. B **651**, 225 (2003).
[9] A. R. Williamson and J. Zupan, Phys. Rev. D **74**, 014003 (2006), Erratum-ibid. D **74**, 03901 (2006).
[10] S. Barshay, D. Rein and L. M. Sehgal, Phys. Lett. B **259**, 475 (1991); A. S. Dighe, M. Gronau and J. L. Rosner, Phys. Rev. Lett. **79**, 4333 (1997); C.-W. Chiang, M. Gronau, J. L. Rosner and D. A. Suprun, Phys. Rev. D **70**, 034020 (2004); H. Wang, X. Liu, Z. Xiao, L. Guo and C.-D. Lu, Nucl. Phys. B **738**, 243 (2006).
[11] S. Kurokawa and E. Kikutani, Nucl. Instr. and Meth. A **499**, 1 (2003), and other papers included in this volume.
[12] Belle Collaboration, A. Abashian *et al.*, Nucl. Instr. and Meth. A **479**, 117 (2002).
[13] Z. Natkaniec *et al.* (Belle SVD2 Group), Nucl. Instr. and Meth. A **560**, 1 (2006).
[14] R. A. Fisher, Ann. Eugenics **7**, 179 (1936).
[15] E. Barberio and Z. Wąs, Comput. Phys. Commun. **79**, 291 (1994); P. Golonka and Z. Was, hep-ph/0506026. We use PHOTOS version 2.13 allowing the emission of up to two photons, with an energy cut-off at 1% of the energy available for photon emission (i.e. approximately 26 MeV for the first emitted photon). PHOTOS also takes into account interference between charged final state particles.
[16] H. Kakuno *et al.*, Nucl. Instr. and Meth. A **533**, 516 (2004).
[17] Belle Collaboration, Y. Chao *et al.*, Phys. Rev. Lett. **93**, 191802 (2004).
[18] ARGUS Collaboration, H. Albrecht *et al.*, Phys. Lett. B **241**, 278 (1990).
[19] W.-M. Yao *et al.* (Particle Data Group), J. Phys. G. **33**, 1 (2006).
[20] G. Nanava and Z. Wąs, hep-ph/0607019.